Journal of ELECTRONIC MATERIALS, Vol. 46, No. 7, 2017
DOI: 10.1007/s11664-017-5357-4


# A Transient Liquid Phase Sintering Bonding Process Using Nickel-Tin Mixed Powder for the New Generation of High-Temperature Power Devices

HONGLIANG FENG,[1] JIHUA HUANG,[1,2] JIAN YANG,[1] SHAOKUN ZHOU,[1] RONG ZHANG,[1] and SHUHAI CHEN[1]

1.—School of Materials Science and Engineering, University of Science and Technology Beijing, 30 Xueyuan Road, Haidian District, Beijing 100083, China. 2.—e-mail: jhhuang62@sina.com

A transient liquid phase sintering (TLPS) bonding process, Ni-Sn TLPS bonding was developed for the new generation of power semiconductor packaging. A model Ni/Ni-Sn/Ni sandwiched structure was assembled by using 30Ni-70Sn mixed powder as the reactive system. The results show that the bonding layer is composed of $Ni_3Sn_4$ and residual fine Ni particles with a small amount of $Ni_3Sn_2$ at 340°C for 240 min, which has a heat-resistant temperature higher than 790°C. The microstructural evolution and thermal characteristic of the bonding layer for various times at 300°C and 340°C were also studied, respectively. This reveals that, after isothermally holding for 240 min at 300°C and for 180 min at 340°C, Sn has been completely transformed into Ni-Sn intermetallic compounds (IMCs) and the bonding layer is mainly composed of $Ni_3Sn_4$ and residual Ni particles. The analysis result for the mechanical properties of the joint shows that the hardness of the bonding layer at 340°C for 240 min is uniform and that the average value reaches 3.66 GPa, which is close to that of the $Ni_3Sn_4$ block material. The shear test shows that, as the holding time increases from 60 min to 180 min at 340°C, because of the existence of Sn, the disparity of shear strength between room temperature and 350°C is large. But when the holding time is 180 min or longer, Sn has been completely transformed into Ni-Sn IMCs. Their performances are very similar whether at room temperature or 350°C.

**Key words:** Bonding, TLPS, high temperature, IMC

## INTRODUCTION

The service temperature of the new generation of semiconductor (SiC, GaN) devices has been demonstrated up to 500°C.[1–3] In order to make full use of the excellent properties of the new generation of semiconductors, the latest trend for packaging the high-temperature power devices is to develop a chip bonding process with the feature of "low-temperature bonding/high-temperature service".[4–9]

In recent years, a process called transient liquid phase sintering (TLPS) bonding has been developed for the packaging of high-temperature power devices. It uses a mixed binary or ternary powder, which includes a metal constituent with a low melting point and which may react with each other to form intermetallic compounds (IMCs) with high melting point, as the filler material. Benefiting from the process principle, the TLPS bonding process exhibits a series of advantages, such as low bonding pressure and temperature, excellent resistance to high temperature, strong adaptability and so on. Up to now, some binary or ternary systems have been introduced and investigated as the reactive system of TLPS bonding, such as Sn-Cu,[10–12] Sn-Ag,[11] Ag-In,[13] Sn-Bi-Cu[14] and Sn-Bi-Ag system.[15] The Sn-Bi-Ag ternary system has been carried out under 200°C for TLPS bonding and the heat-resistant

(Received August 25, 2016; accepted February 3, 2017; published online February 17, 2017)

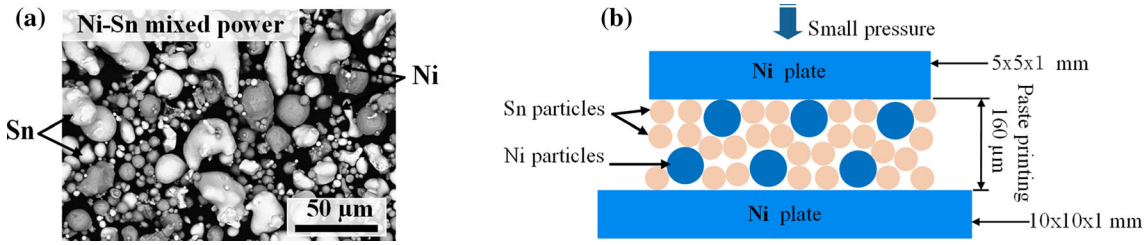


Fig. 1. Ni-Sn mixed power and schematics of TLPS bonding: (a) Ni-Sn mixed power; (b) initial arrangement.

temperature reaches up to 250°C.[15] Furthermore, using the Sn-Cu system, SiC devices can be bonded under a pressure of 0.3 MPa at 260°C. Meanwhile, the shear strength of the bond can reach about 40 MPa tested at 300°C,[10] which shows that TLPS bonding has great potential for high-temperature resistance packaging.

It is understood from the principle of TLPS bonding that the assistant pressure depends on the amount of the liquid formed during the bonding process: the more liquid that exists, the less assistant pressure is required. The temperature resistance of the bonding layer is decided by the melting temperature of the formed IMCs: the higher melting the temperature of the IMCs, the higher the temperature resistance of the bonding layer. According to the Ni-Sn phase diagram,[16] the Ni-Sn binary system has an IMC of $Ni_3Sn_4$ close to the Sn side, which has a melting temperature of 794.5°C. This means that the Ni-Sn system as the reactive system may possess more liquid and better bonding characteristics than Cu-Sn, Ag-In and Ag-Sn systems. In this work, the Ni-Sn system was employed as the reactive system to develop a TLPS bonding process for the packaging of the new generation of power devices. A model Ni/Ni-Sn/Ni sandwiched structure was assembled by using 30Ni-70Sn mixed powder as the reactive system of TLPS. The microstructure, interface structure and temperature resistance of the Ni-Sn TLPS bonding layer under different processes were studied and the process node of the microstructural evolution behavior was given ulteriorly. Meanwhile, the shear tests of the joints, conducted at room temperature and high temperature (350°C), have been discussed in detail.

## EXPERIMENTAL

A Ni/Ni-Sn/Ni sandwiched simulation package structure was assembled by using 30Ni-70Sn (wt.%) mixed powder as the bonding material. Before the assembly, the Ni plates were cut into small pieces with dimensions of 10 mm × 10 mm × 1 mm and 5 mm × 5 mm × 1 mm. The Ni-Sn mixed powder was composed of high-purity nickel powder with an average particle size of 10 $\mu$m and high-purity tin powder with a particle size of 5–20 $\mu$m, as shown in Fig. 1a. The two kinds of powders were evenly mixed with alcohol and then printed and placed between the Ni plates, assembled into a sandwiched structure, as shown in Fig. 1b. The Ni/Ni-Sn/Ni sandwich sample was quickly heated up to 300°C and 340°C with a heating rate of 80°C/min and 0.1 MPa bonding pressure in a vacuum furnace (vacuum degree $<10^{-3}$ Pa), followed by an isothermal hold for different times. After the isothermal process, the bonding structure was cooled to room temperature by the blowing treatment of high-purity argon gas.

The microstructures were characterized by a scanning electron microscope (SEM) equipped with energy dispersal x-ray (EDX) spectroscopy. The crystal structure of each phase was identified by x-ray diffraction (XRD) and a transmission electron microscope (TEM) with energy dispersal x-ray (EDX) spectroscopy. The phase transformation was analyzed by differential scanning calorimetry (DSC) in a constant heating rate of 10°C/min. The shear strength was measured using a shear machine with the shear speed of 20 $\mu$m/s at room temperature and 350°C. The hardness of the bonding layer was determined by a Vickers hardness test machine with the load quality of 50 g.

## RESULTS AND DISCUSSION

### Microstructure and Interface Structure of Ni-Sn TLPS Bonding Layer

Figure 2 shows the cross-sectional SEM image, XRD pattern analysis and the elements line scanning of the Ni-Sn TLPS bonding layer after a 240-min hold time at 340°C. It shows that the Ni plates were perfectly bonded together and a dense bonding layer was achieved, as presented in Fig. 2a. The XRD pattern analysis and the elements Ni and Sn line scanning of the bonding layer indicate that it is mainly composed of $Ni_3Sn_4$ and residual fine Ni particles which may play a role in increasing the toughness of the bonding layer, as shown in Fig. 2b and c. It is worth noting that there are many residual Ni particles in the bonding layer. Based on the analysis, it was found that the ratio of Ni and Sn in the original Ni-Sn mixed powder was 30:70 which is only slightly larger than that in $Ni_3Sn_4$ (28:72). Therefore, it has been concluded that a considerable amount of Ni from the Ni plates was dissolved into the bonding layer. It can also be seen that the elements Ni and Sn are distributed uniformly, and therefore the $Ni_3Sn_4$ intermetallic compound is also very uniform in the bonding layer.

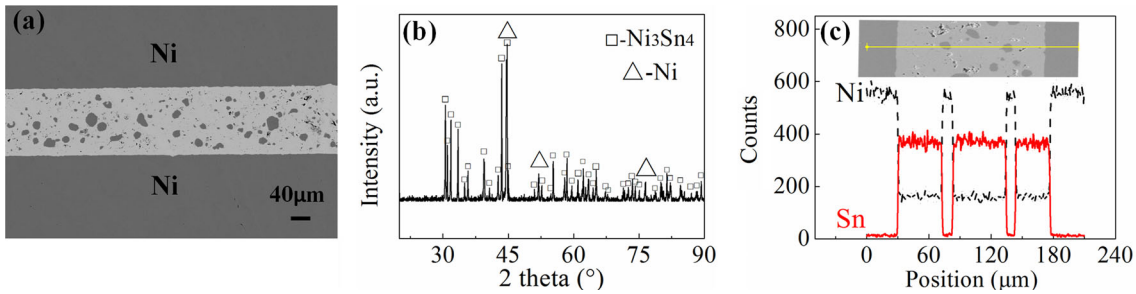


Fig. 2. SEM image of the Ni-Sn TLPS bonding layer: (a) the cross-sectional image, (b) XRD pattern and (c) element distribution of the bonding layer.

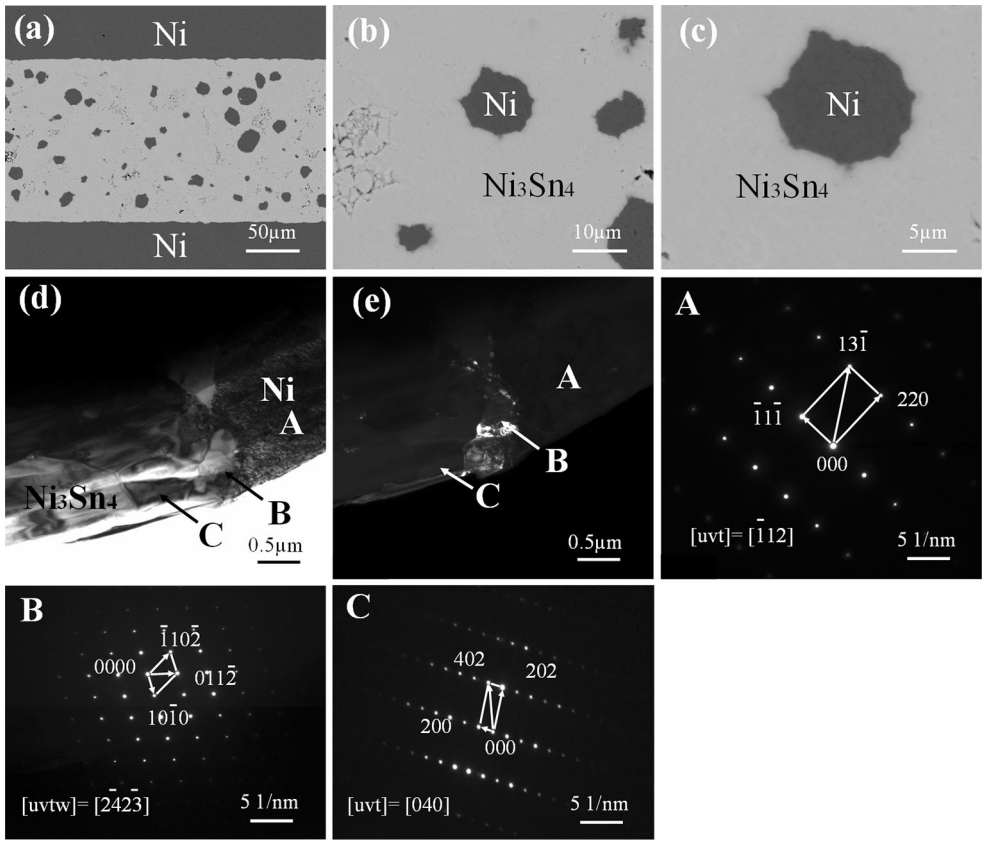


Fig. 3. SEM and TEM images of the bonding layer bonded at 340°C for 240 min: (a) cross-sectional image; (b) and (c) are locally amplified images; (d) further amplified TEM bright field image and (e) dark field image of interface between the Ni-Sn compound and the Ni particles. Inset corresponding SAD patterns: *A* Ni, *B* $Ni_3Sn_2$ and *C* $Ni_3Sn_4$.

Figure 3 illustrates the interfacial phase structure of the Ni-Sn TLPS bonding layer bonded at 340°C for 240 min. By a series of locally amplified SEM images (Fig. 3a–c), it can be seen that the $Ni_3Sn_4$ intermetallic compound around the Ni particles does not have any obvious distinction. The further amplified TEM bright field image and dark field image of the interface are shown in Fig. 3d and e. They show that very little of the $Ni_3Sn_2$ compound has formed in the interface between the Ni particles and the $Ni_3Sn_4$ compound and that the bonding layer is mainly composed of $Ni_3Sn_4$ and residual fine Ni particles. The selected-area diffraction (SAD) patterns of the right-hand are calibrated in the areas marked A, B and C. From the calibrated diffraction patterns and the EDX spectroscopy analysis (in Table I), A presents a face-centered cubic lattice with the composition of 99.02 at.% Ni and 0.97 at.% Sn, while B and C present a hexagonal lattice and a monoclinic lattice with the composition of 62.99 at.% Ni and 37.00 at.% Sn, 40.28 at.% Ni and 59.71 at.% Sn, which indicates that A, B and C are Ni, $Ni_3Sn_2$ and $Ni_3Sn_4$, respectively. Therefore, it can be concluded that

**Table I. The chemical composition (in at.%) of the interface in Fig. 3d measured by EDX spectroscopy**

| The marked areas | Crystal | Ni | Sn | Phase |
|---|---|---|---|---|
| A | Face-centered cubic | 99.02 | 0.97 | Ni |
| B | Hexagonal | 62.99 | 37.00 | $Ni_3Sn_2$ |
| C | Monoclinic | 40.28 | 59.71 | $Ni_3Sn_4$ |

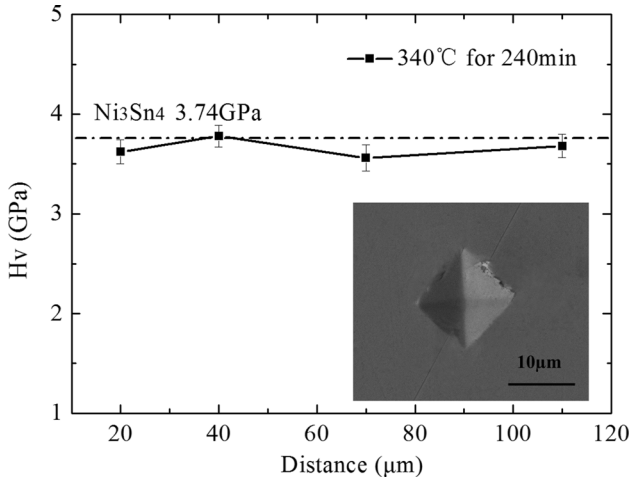


Fig. 4. Vickers hardness of the Ni-Sn TLPS bonding layers variation as a function of the distance to the bonding layer boundary. Inset Vickers hardness indentation on bonding layer.

the bonding layer is composed of $Ni_3Sn_4$ and residual fine Ni particles with a small amount of $Ni_3Sn_2$ at 340°C for 240 min. As indicated in the Ni-Sn phase diagram,[16] the melting temperature of $Ni_3Sn_4$ IMC is close to 800°C and that of $Ni_3Sn_2$ is as high as 1280°C. Therefore, the Ni-Sn TLPS bond has very high heat resistance temperature.

The Vickers hardness of the bonding layer after a 240-min hold time at 340°C was measured and the results are shown in Fig. 4. The boundary of the bonding layer was made as the starting point of measurement. The hardness at different positions of 20 $\mu$m, 40 $\mu$m, 70 $\mu$m, and 110 $\mu$m was measured. Each average value was measured by three samples and the figure inset shows the Vickers hardness indentation on the bonding layer. The results show that the hardness values of the different positions are similar and that the average hardness value of the compound is 3.66 GPa, which is very close to the 3.74 GPa of the block $Ni_3Sn_4$, indicating that the Ni-Sn bonding layer is uniform and dense.

## Microstructural Evolution and Thermal Characteristic of Ni-Sn TLPS Bonding Layer

The microstructural evolution and thermal characteristic of the TLPS bonding layer at 300°C and 340°C for different times were further studied and the results are shown in Figs. 5, 6, 7, and 8. After holding for 20 min and 60 min at 300°C, the bonding layer still contains a large amount of unreacted Sn, as shown in Fig. 5a and b. For a short hold time, because of the presence of a large amount of Sn in the bonding layer and because the melting point of Sn is low, the bonding layer cannot be served at a higher temperature. Therefore, only after a longer hold time, when the Sn has been completely transformed into the high-melting point Ni-Sn compounds, the bonding layer would have high-temperature resistance. Further extending the hold time to 120 min and 180 min, the Ni reacted with the Sn and was further transformed into $Ni_3Sn_4$ IMC, but there is still little remaining Sn in the bonding layer, as shown in Fig. 5c and d. The DSC trace of the original Sn powder shows that there is an endothermic peak at 231.6°C, as shown in Fig. 6a. After holding for 180 min, the endothermic peak of Sn becomes weaker and the endothermic peak of $Ni_3Sn_4$ becomes stronger, as shown in Fig. 6b. This confirms that the Ni and Sn react incompletely and that there is still some residual Sn in the bonding layer. But when the hold time extends to 240 min, Sn no longer exists in the bonding layer observed by SEM, as shown in Fig. 5e. The DSC trace further confirms that the Sn has been completely transformed into Ni-Sn IMCs in the bonding layer at 300°C for 240 min, as shown in Fig. 6c. This means that after 240 min the bonding layer is mainly composed of $Ni_3Sn_4$ and residual fine Ni particles, which has a heat-resistant temperature higher than 790°C.

Figure 7 illustrates the microstructural evolution of the TLPS bonding layer at 340°C for different times. From Fig. 7a and b, it can be seen that after 20 min and 60 min at 340°C, there is a large amount of $Ni_3Sn_4$ and much residual Sn in the bonding layer. Combined with the DSC analysis of Fig. 8a, this shows that there is a endothermic peak of Sn at 234.5°C and the other endothermic peak of $Ni_3Sn_4$ starting from 799.9°C has appeared, which confirms that an amount of $Ni_3Sn_4$ has formed in the bonding layer after 60 min. Further prolonging the hold time to 120 min, the content of Sn in the bonding layer decreases (Fig. 7c). This phenomenon has also been confirmed by the DSC analysis of Fig. 8b, in which the endothermic melting peak of Sn is decreased and the heat endothermic peak of $Ni_3Sn_4$ is remarkably enhanced. Continuing to

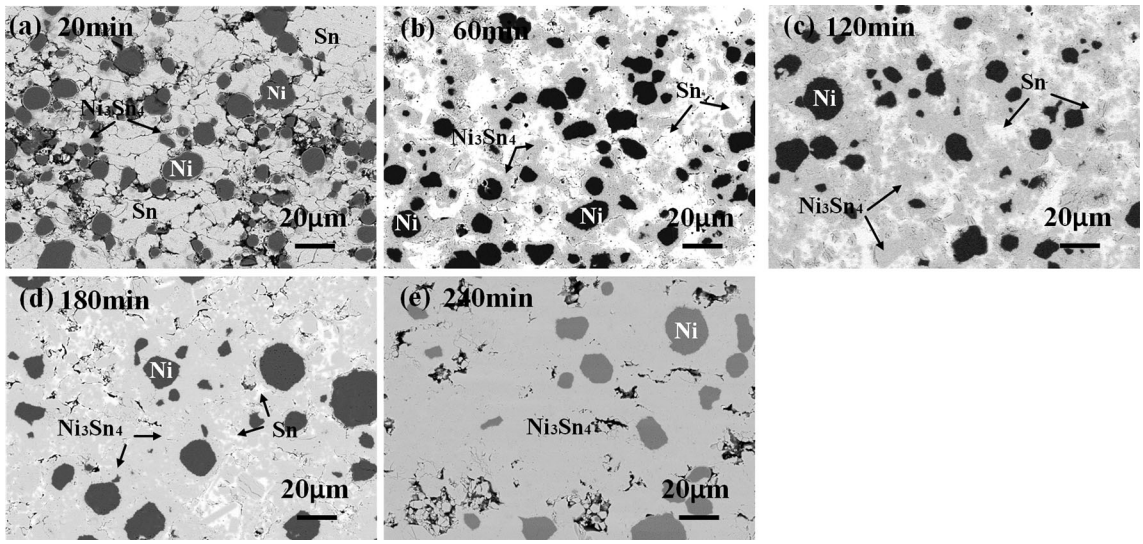


Fig. 5. SEM images of the Ni-Sn TLPS bonding layer isothermally holding for different times at 300°C: (a) 20 min; (b) 60 min; (c) 120 min; (d) 180 min; and (e) 240 min.

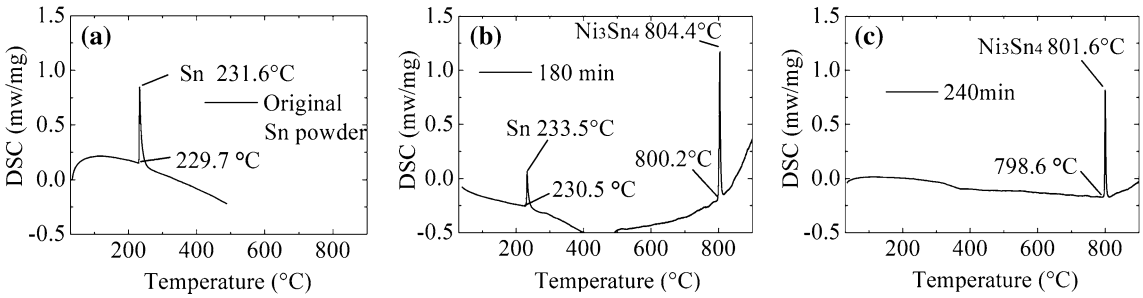


Fig. 6. DSC traces of the bonding layers isothermally holding for different times at 300°C: (a) original Sn powder; (b) 180 min; and (c) 240 min.

extend the hold time to 180 min, the Sn has been completely transformed into the high-melting point Ni-Sn compounds, as shown in Fig. 7d. Meanwhile, the Sn endothermic peak has disappeared and the intensity of the $Ni_3Sn_4$ peak is constantly improving, as shown in Fig. 8c. This feature indicates that the Sn has been completely transformed into Ni-Sn IMCs (almost entirely of $Ni_3Sn_4$) with a processing hold time of 180 min.

## Mechanical Property and Fracture Morphology of Ni-Sn TLPS Bonding Layer

The shear test of the joints bonded at 340°C for different times were conducted at both room temperature and high temperature (350°C). Each group included four shear samples in the same process and they were tested and the average value taken. As shown in Fig. 9, the shear strength of the joint increases with the increasing hold time from 60 min to 150 min at room temperature. For the joint with the holding time of 60 min, at the position of $Ni_3Sn_4$ (point A), it shows a brittle fracture characteristic, as shown in Fig. 10, which is the fracture morphologies after the typical time periods. Table II shows the energy spectra in the marked areas. As shown in Fig. 10 and Table II, there is also much relatively soft Sn around the $Ni_3Sn_4$ (point B), due to the weakness of Sn in the bonding layer, so the strength is relatively low. When the hold time increases to 120 min,the Sn in the bonding layer is relatively small and the bonding layer has a large amount of hard $Ni_3Sn_4$ and therefore the shear strength of the joint is increased. Finally, when the hold time is 180 min or longer (240 min and 300 min), the DSC traces (Fig. 7) and the fracture (Fig. 10c) show that the Sn has disappeared and been completely transformed into hard Ni-Sn IMCs. As the bonding layer has been completely transformed into brittle Ni-Sn IMCs which is very

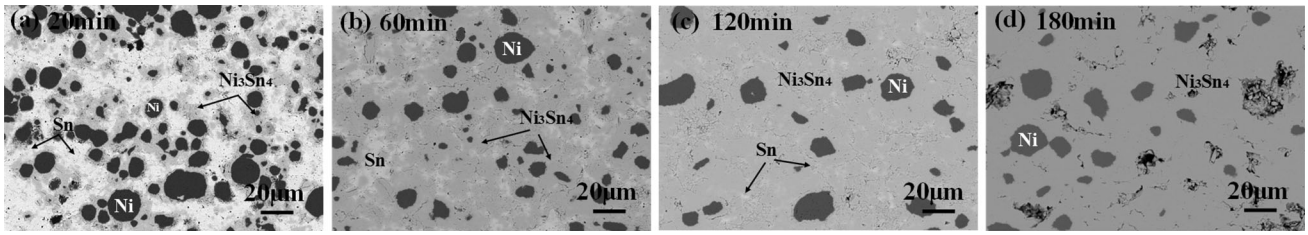


Fig. 7. SEM images of the Ni-Sn TLPS bonding layer isothermally holding for different times at 340°C: (a) 20 min; (b) 60 min; (c) 120 min; and (d) 180 min.

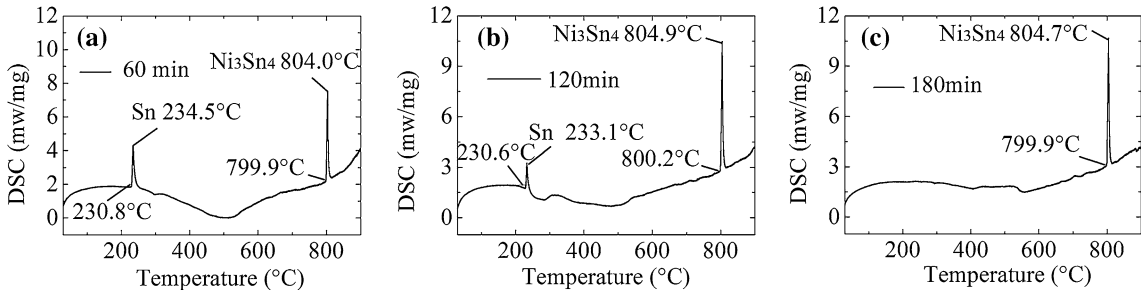


Fig. 8. DSC traces of the bonding layers isothermally holding for different times at 340°C: (a) 60 min; (b) 120 min; and (c) 180 min.

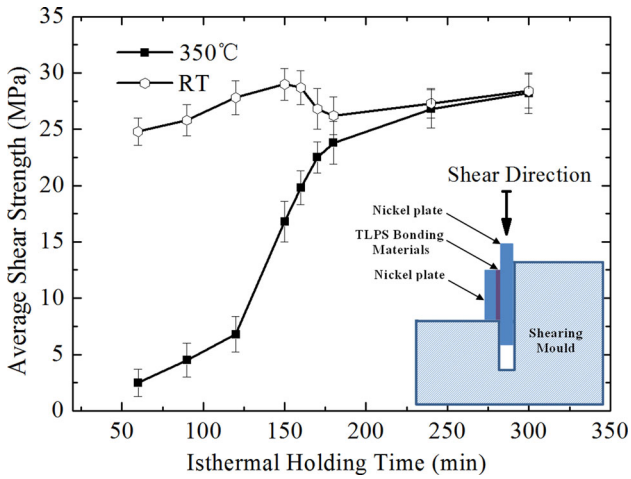


Fig. 9. Shear strength of Ni-Sn TLPS bonding layers variation as a function of hold times, tested at room temperature and 350°C.

sensitive to cracks, when the Sn has completely disappeared, the shear strength decreases slightly and then tends to be stable.

For the shear test at 350°C, Sn has melted in the fracture of joint bonded at 340°C for 60 min, as shown in Fig. 11a. This very clearly confirms that the fracture occurs in the melting Sn determined by the energy spectrum of point D (in Table III), so the shear strength of the bonding layer is very small. When the hold time is extended to 120 min, most of the Sn has been transformed into Ni-Sn IMCs but there still exists a small amount of Sn. Due to the melting of the Sn dispersed in the $Ni_3Sn_4$, the $Ni_3Sn_4$ in the bonding layer is relatively loose at high temperature (Fig. 11b and f), so the shear strength of the bonding layer is low. But when the hold time is increased from 180 min to 300 min, Sn has been completely transformed into the hard high-melting point Ni-Sn IMCs (almost entirely of $Ni_3Sn_4$), as shown in Figs. 8 and 11c. Therefore, no matter whether at 350°C or room temperature, the fracture morphologies are very similar, which leads to a similar shear strength.

Comparative analysis of the strength results at room temperature and high temperature. It is worth noting that for a hold time from 60 min to 180 min at 340°C, because of the existence of the Sn, the disparity of shear strength between high temperature and room temperature is large. But when the hold time is 180 min or longer (240 min and 300 min), the Sn has been completely transformed into hard high-melting point Ni-Sn IMCs. Whether at room temperature or high temperature at this time, their performances are very similar—fracture occurred at the dense $Ni_3Sn_4$ without obvious difference and the strength disparity is also very small, as shown in Figs. 9, 10c, and 11c. The average shear strength of the joint at 340°C for 300 min is up to 28.2 MPa (test at 350°C), which is very close to that at room temperature, at 28.5 MPa. Therefore, the temperature resistance is obvious. After the research of Ni-Sn TLPS bonding, it ihas been proved that the Ni-Sn TLPS bonding process is a very potential low-temperature bonding/high-temperature service process.

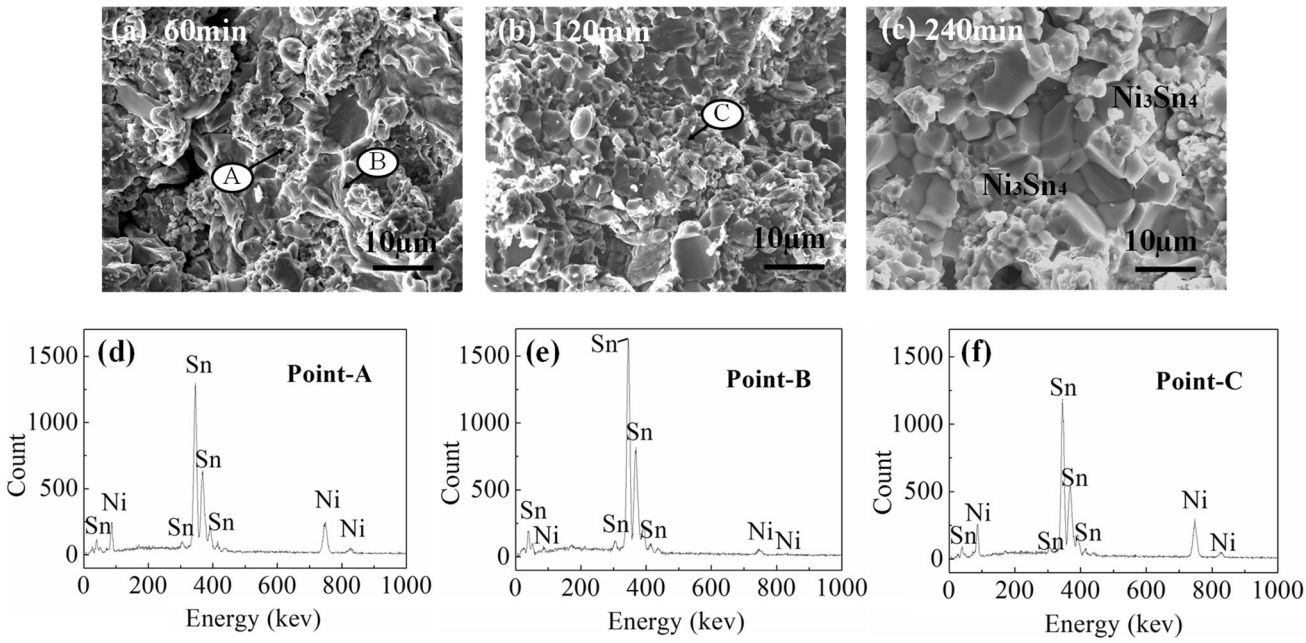


Fig. 10. Typical shear fracture morphologies of the Ni-Sn TLPS bonding layers bonded at 340°C for different times, tested at room temperature: (a) 60 min; (b) 120 min; and (c) 240 min. EDX spectra of each marked point: (d) *Point A*; (e) *Point B*; and (f) *Point C*.

**Table II. The chemical composition (in at.%) of each marked point in Fig. 10 measured by EDX spectroscopy**

| The marked points | Ni | Sn | Phase |
|---|---|---|---|
| Point A | 44.05 | 55.95 | $Ni_3Sn_4$ |
| Point B | 6.31 | 93.69 | Sn |
| Point C | 43.88 | 56.12 | $Ni_3Sn_4$ |

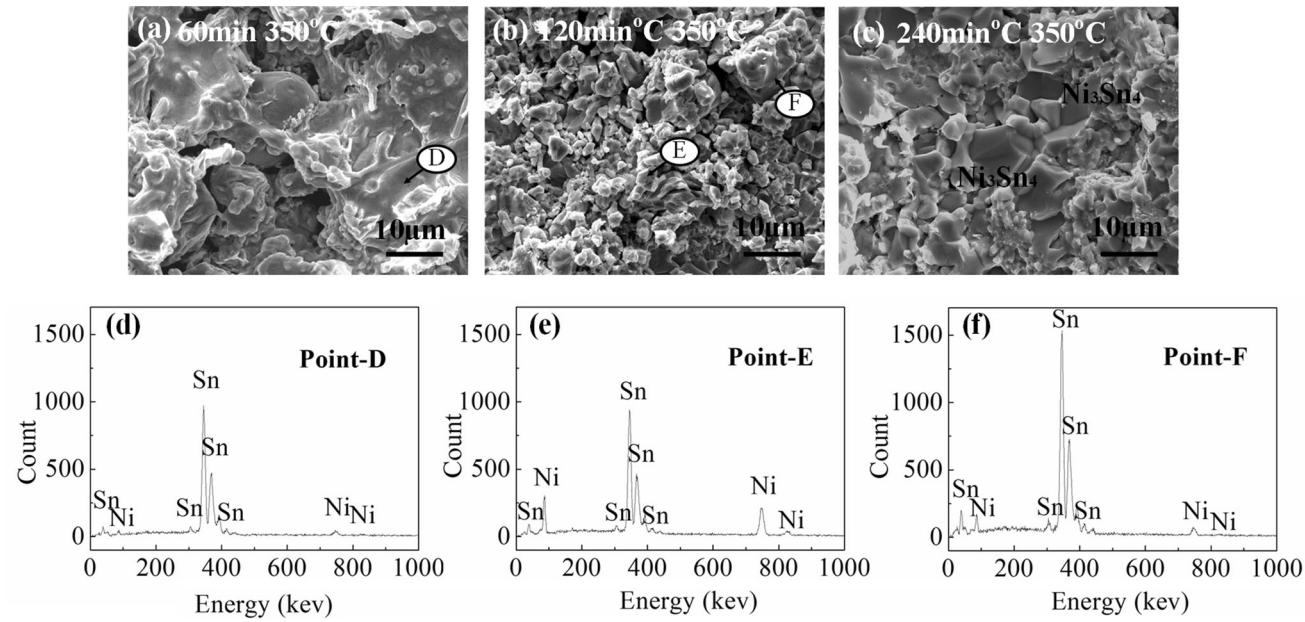


Fig. 11. Typical shear fracture morphologies of the Ni-Sn TLPS bonding layers bonded at 340°C for different times, tested at 350°C: (a) 60 min; (b) 120 min; and (c) 240 min. EDX spectra of each marked point: (d) *Point D*; (e) *Point E* and (f) *Point F*.

**Table III. The chemical composition (in at.%) of each marked point in Fig. 11 measured by EDX spectroscopy**

| The marked points | Ni | Sn | Phase |
|---|---|---|---|
| Point D | 3.84 | 97.16 | Sn |
| Point E | 41.11 | 58.89 | $Ni_3Sn_4$ |
| Point F | 8.84 | 91.16 | Sn |

## CONCLUSION

In summary, a model Ni/Ni-Sn/Ni sandwiched structure was successfully assembled by using 30Ni-70Sn mixed powder as the reactive system of TLPS for the new generation of power semiconductor packaging. After holding for 240 min at 340°C, the bonding layer is composed of $Ni_3Sn_4$ and residual fine Ni particles with a small amount of $Ni_3Sn_2$, which has a heat-resistant temperature higher than 790°C. The evolution of the microstructure of the bonding layer isothermally holding for different times at 300°C and 340°C was studied. It was found that after isothermally holding for 240 min at 300°C and for 180 min at 340°C under a pressure of 0.1 MPa, respectively, Sn has been completely transformed into Ni-Sn IMCs. Further analysis of the mechanical properties of the bonding layer, found that the hardness of the bonding layer for 240 min at 340°C is uniform and that the average value can reach 3.66 GPa, very close to the $Ni_3Sn_4$ hardness. The shear strength increases with the increase of holding time, tested at room temperature and 350°C, and it is worth noting that, for a hold time from 60 min to 150 min at 340°C, because of the existence of Sn, the disparity of shear strength between room temperature and high temperature is large. But when the hold time is 180 min or longer (240 min and 300 min), Sn has been completely transformed into hard high-melting point Ni-Sn IMCs. No matter whether at room temperature or high temperature at this time, their performances are very similar—fracture occurred in the dense $Ni_3Sn_4$ without any obvious difference. Therefore, the Ni-Sn TLPS bonding process is a very promising low-temperature bonding/high-temperature service process.

## ACKNOWLEDGEMENTS

This work is supported by National Nature Science Foundation of China under Grant No. 51474026. The authors acknowledge Li You Engineer and De-min Liu senior engineer for their assistances in TEM analysis and high-temperature shear test.

## REFERENCES

1. R. Hedayati, L. Lanni, and S. Rodriguez, *IEEE Electron Device Lett.* 35, 693 (2014).
2. D. Maier, M. Alomari, N. Grandjean, J. Carlin, M. Diforte-Poisson, C. Dua, S. Delage, and E. Kohn, *IEEE Electron Device Lett.* 33, 985 (2012).
3. P.G. Neudeck, S.L. Garverick, and D.J. Spry, *Phys. Status Solidi A* 206, 2329 (2009).
4. N.S. Bosco and F.W. Zok, *Acta Mater.* 53, 2019 (2005).
5. S. Wang, M.Y. Li, and H.J. Ji, *Scr. Mater.* 69, 789 (2013).
6. T. Luu, A. Duan, K.E. Aasmundtvit, and N. Hoivik, *J. Electron. Mater.* 42, 3582 (2013).
7. Y. Yen, W. Liou, H. Wei, and C. Lee, *J. Electroact. Mater.* 38, 93 (2009).
8. A. Hu, J.Y. Guo, H. Alarifi, G. Patane, Y. Zhou, G. Compagnini, and C.X. Xu, *Appl. Phys. Lett.* 97, 153117 (2010).
9. S.J. Wang, L.H. Hsu, N.K. Wang, and C.E. Ho, *J. Electroact. Mater.* 43, 219 (2013).
10. F.Q. Lang, H. Yamaguchi, H. Nakagawa, and H. Sato, *Electrochem. Soc.* 160, 315 (2013).
11. H. Greve and F.P. McCluskey, in *Proceedings of ASME 2013*, Burlingame, California (2013).
12. J. Bultitude, J. McConnell, and C. Shearer, *J. Mater. Sci. Mater. Electron.* 26, 9236 (2015).
13. P.O. Quintero and F.P. McCluskey, *J. Microelectron. Electron.* 6, 66 (2009).
14. T. D'hondt and S.F. Corbin, Metall. *Mater. Trans.* 37A, 217 (2006).
15. I. Ohnuma, R. Kainuma, and K. Ishida, *J. Min. Metall. B.* 48, 413 (2012).
16. H. Okamoto, *J. Phase Equilib. Diffus.* 29, 297 (2008).